

## **Timescale Correlation between Marine Atmospheric Exposure and Accelerated Corrosion Testing – Part 2**

Eliza L. Montgomery  
NASA Postdoctoral Program  
Mail Code: NE-L2  
Kennedy Space Center, FL 32899

Jerome C. Curran  
ESC – Team QNA  
Mailstop ESC 24  
Kennedy Space Center, FL 32899

Luz Marina Calle  
NASA  
Mail Code: NE-L2  
Kennedy Space Center, FL 32899

Mark R. Kolody  
ESC – Team QNA  
Mailstop ESC 24  
Kennedy Space Center, FL 32899

### **ABSTRACT**

Evaluation of metals to predict service life of metal-based structures in corrosive environments has long relied on atmospheric exposure test sites. Traditional accelerated corrosion testing relies on mimicking the exposure conditions, often incorporating salt spray and ultraviolet (UV) radiation, and exposing the metal to continuous or cyclic conditions similar to those of the corrosive environment. Their reliability to correlate to atmospheric exposure test results is often a concern when determining the timescale to which the accelerated tests can be related. Accelerated corrosion testing has yet to be universally accepted as a useful tool in predicting the long-term service life of a metal, despite its ability to rapidly induce corrosion. Although visual and mass loss methods of evaluating corrosion are the standard, and their use is crucial, a method that correlates timescales from accelerated testing to atmospheric exposure would be very valuable. This paper presents work that began with the characterization of the atmospheric environment at the Kennedy Space Center (KSC) Beachside Corrosion Test Site. The chemical changes that occur on low carbon steel, during atmospheric and accelerated corrosion conditions, were investigated using surface chemistry analytical methods. The corrosion rates and behaviors of panels subjected to long-term and accelerated corrosion conditions, involving neutral salt fog and alternating seawater spray, were compared to identify possible timescale correlations between accelerated and long-term corrosion performance. The results, as well as preliminary findings on the correlation investigation, are presented.

Key words: atmospheric exposure, accelerated corrosion testing, alternating seawater spray, marine, correlation, seawater, carbon steel, long-term corrosion performance prediction, X-ray photoelectron spectroscopy.

## INTRODUCTION

Lifetime service prediction of metal-based structures has historically been based on corrosion performance at atmospheric exposure corrosion test sites. This real-time corrosion environment exposure requires a long time, often 3-5 years at a minimum, and usually relies on visual and weight loss methods to quantify the degree of corrosion of a particular metal in a specific environment. These methods are common and necessary. There is no question that the development of an accelerated method that successfully correlates results from accelerated corrosion tests to those obtained from long-term atmospheric exposure would be very valuable.<sup>1-4</sup> The development of degradation models, accelerated test methods, and other atmospheric correlations to real-time atmospheric exposure is a great challenge.<sup>1-11</sup> To date, no accelerated method has been successful in correlating atmospheric exposure data to be considered satisfactory for universal use. Currently, a solution to that challenge is nearly inconceivable due to all the different parameters that must be considered.

The variables involved in predicting atmospheric corrosion in any specific environment, such as temperature, pollutants, and moisture, dictate that accelerated corrosion techniques must be tailored for each end-use environment.<sup>1,4,6,12-15</sup> Previous papers<sup>16,17</sup> have provided a review of various challenges associated with correlating results obtained from accelerated corrosion techniques to those from atmospheric corrosion, primarily for steels in marine environments. These papers also provided a historical review of past work involving the most common accelerated corrosion test methods, along with past work in characterizing marine-induced iron corrosion products. Environmental variables within different corrosion environments have been studied by others.<sup>12,14,16-18</sup> The unique natural environment at the Kennedy Space Center (KSC), which includes sea-salt, moisture, and intermittent exposure to rocket exhaust, has yet to be fully understood. The manner in which spaceport structures degrade is known to a degree, but degradation must be more completely understood in order to develop methods to predict their corrosion performance.

The objective of the work presented on this paper is to determine correlations between corrosion performance obtained with accelerated corrosion testing methods and with long-term atmospheric exposure at the KSC's Beachside Atmospheric Corrosion Test Site. KSC is known to be one of the most corrosive places in North America<sup>19</sup> and characterization of this site is a crucial step for the investigation of accelerated corrosion tests correlations to long-term performance. Environmental factors, including monthly chloride and sulfur dioxide concentration, weather conditions, and wave height, have been chosen to characterize this site. Corrosion rates for 1010 steel (UNS 10100) have been monitored for each corrosion environment to determine general correlations. The initial corrosion product formation is hypothesized to be an important factor in interpreting correlation discrepancies. Both visual and surface chemistry analytical techniques were used to investigate initial corrosion product formation.

### Challenges at NASA Kennedy Space Center

NASA KSC's Beachside Corrosion Test Site has been documented as the most corrosive place known in the United States.<sup>19</sup> Figure 1 displays the location of KSC and the beachside test site along Florida's Atlantic coast. The environmental challenges at KSC are both natural and man-made. The already higher-than-typical aggressive marine conditions are intermittently enhanced by the emission of 70 tons of hydrochloric acid into the atmosphere during launches that use rockets with solid fuel. Correlating corrosion rates from accelerated corrosion methods and real-time beachside atmospheric exposure at KSC is challenged largely by marine effects such as the type and time of wetness and chloride deposition. Despite the corrosive environment, launch structures are largely made using structural steel, namely AISI 1010 (UNS G1010). Different coatings, such as sacrificial coatings and paints, are used to slow corrosion. Current coating qualifications at KSC depend largely on a material's performance during atmospheric corrosion conditions for 18 months and ultimately a 5-year-period<sup>20</sup> This testing, while necessary, is very time consuming when qualifying new materials. A testing protocol is needed to accelerate the material qualification time. Identifying correlations between accelerated



corrosion and atmospheric corrosion timescales for KSC-specific environmental conditions is a logical step towards that goal.

## EXPERIMENTAL PROCEDURES

### Test Plan Summary

Topics addressed in this study of corrosion conditions at KSC include:

- 1) Determining the degree of correlation between the corrosion test methods and, perhaps more importantly, the reasons why the different methods may not correlate.
- 2) Identifying the initial corrosion products and composition formed during the different accelerated and long-term corrosion conditions.
- 3) Determining general seasonal-based changes in corrosion product formation for the methods that involve exposure to atmospheric conditions.

This paper is based on work that is currently ongoing. Table 1 displays the techniques that are being used in the current test plan.

**Table 1**  
**Experimental Test Plan Summary**

Purpose	Corrosion Conditions	Analytical Techniques
Corrosion rate correlation	AE <sup>(1)</sup> , ASST <sup>(2)</sup> , B117 <sup>(3)</sup>	Corrosion rate by weight loss methods, chloride concentration
Initial corrosion product formation	AE, ASST, B117	XPS, photo-microscopy
Seasonal effects on corrosion rate	AE, ASST	XPS, microscopy, chloride and sulfur dioxide concentration, corrosion rate by weight loss method, wave height

<sup>(1)</sup> Atmospheric Exposure

<sup>(2)</sup> Alternating Seawater Spray Test

<sup>(3)</sup> ASTM B117<sup>21</sup> method, used during accelerated neutral salt spray method

### Exposure Conditions

For atmospheric exposure testing, 1010 steel (UNS 10100) panels were placed at 30-degree angles towards the Atlantic Ocean at KSC's beachside corrosion test site. The test racks are located 100 feet from the high tide line, Figure 1. The panels were exposed using the following regimes: one-year, monthly (new panels exposed for a month beginning every consecutive month), and monthly successive exposure (a set of panels was exposed at the beginning and subsets of panels were removed and evaluated every consecutive month). The monthly exposure was designed to compare seasonal influences throughout the year and the monthly successive exposure was designed to look at the cumulative effect of corrosion product formation. For accelerated seawater spray testing, 1010 steel panels were placed at 30-degree angles in a seawater spray system, shown in Figure 2, and exposed to atmospheric conditions continuously and to sea spray conditions in cycles for 10 minutes every hour. The panels were exposed during 30, 60, 120, and 180-day periods. For neutral salt fog chamber testing, 1010 steel (UNS 10100) panels were placed in a neutral salt fog chamber in 5% NaCl, using the ASTM<sup>(4)</sup> B117<sup>21</sup> method. The panels were exposed at 100, 250, 470, 500, 750, 1000, 1500, and 1900 hours. The weight loss method in ASTM G1<sup>22</sup> was used to measure corrosion rates for all panels.

<sup>(4)</sup> ASTM International, Conshohocken, PA, USA



## Surface Analysis

X-ray photoelectron spectroscopy (XPS), using an Al K-alpha X-ray source, was used to determine the types of corrosion products formed on the surface of the panels for the different corrosion conditions. In some cases, depth profiles were measured for typical iron, carbon, oxygen, and chloride peak ranges with an ion energy of 3000eV at a rate of 0.37nm/s for 15 seconds per etch.

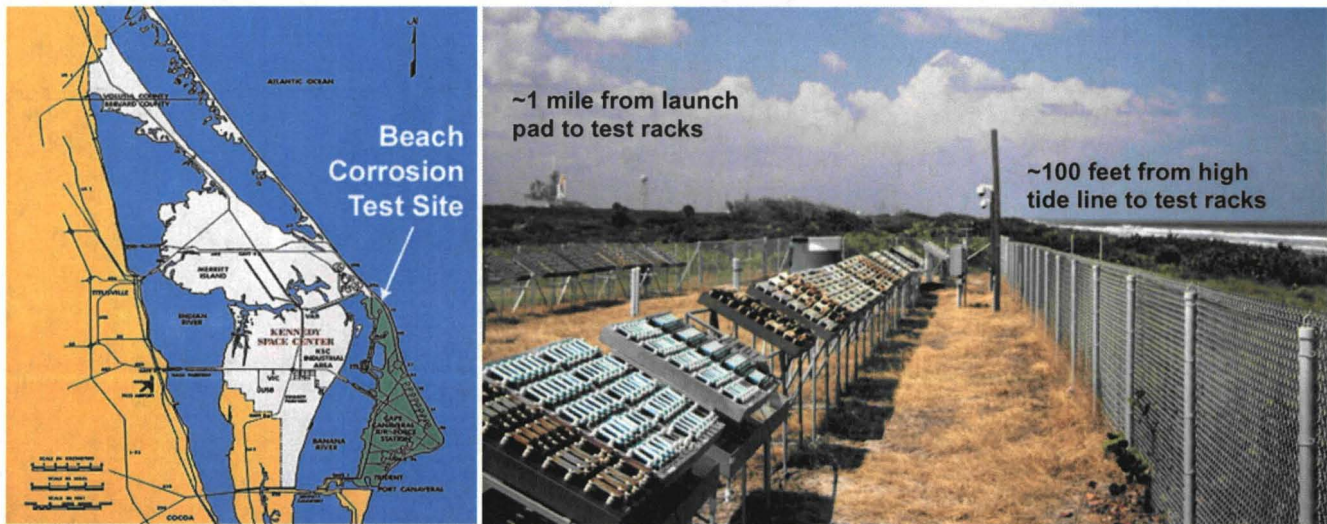


**Figure 1: Location of NASA Kennedy Space Center's Beachside Corrosion Test Site along the Atlantic Ocean (left) and panels exposed to the marine atmosphere at KSC (right).**



**Figure 2: Alternating Seawater Spray system with exposure panels, and modification for panels used for surface analysis (left). Wet candles exposed to KSC beachside atmospheric conditions and used to measure chloride concentration per month (right).**

## Atmospheric Conditions

The temperature, relative humidity, and total precipitation values are recorded at the Beachside Atmospheric Test Site continuously. The precipitation values are measured as a total amount collected every 20 minutes and the temperature and relative humidity are measured every twenty minutes. Chloride deposition at the site is being monitored continuously during the exposure period using the wet candle method.<sup>23</sup> Two replicates of each set are exposed for a one-month period before replacement. The two different sets are exposed in staggered time periods that are two weeks apart. Chloride concentration is measured using a chloride ion probe. Figure 2 shows the wet candle exposure alongside the beachside panel exposure. Sulfur concentration, in the form of sulfur dioxide and



sulfates, was measured through the National Atmospheric Deposition Program (NADP) monitoring location FL99, which is located at the Kennedy Space Center and operated by NASA. The sulfur deposition data is taken from the NADP database website.<sup>24</sup> Wave height measurements were collected from a weather buoy, buoy #41009, off the coast of Cape Canaveral that is funded by NASA and operated by the National Oceanic and Atmospheric Administration's (NOAA) National Data Buoy Center. The wave height data was extracted from the database website.<sup>25</sup> Figure 3 shows the physical location where the sulfur dioxide concentration (S), chloride concentration (Cl<sup>-</sup>), and wave height values are measured.

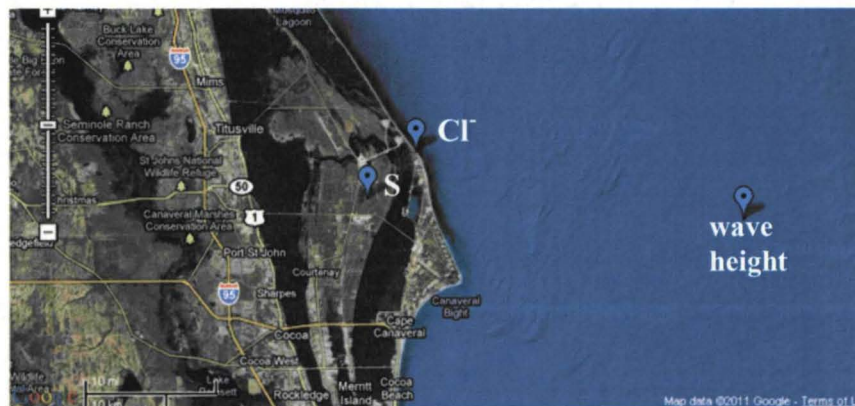


**Figure 3: Map of physical locations where the chloride concentration, sulfur concentration, and wave height values are obtained.**

## RESULTS AND DISCUSSION

The investigation to identify correlations between the different corrosion conditions of atmospheric exposure, ASST, and neutral salt fog, began with a characterization of the atmospheric environment at KSC's Beachside Corrosion Test Site. The corrosion behavior of the 1010 steel panels in the long term and accelerated environments was investigated by determining the corrosion rate and using visual and XPS methods to identify the initial corrosion products.

### Characterization of Beachside Atmospheric Exposure Site

In order to understand the highly corrosive conditions of the natural environment at KSC, various environmental factors such as temperature, relative humidity, precipitation, chloride and sulfur dioxide concentration, and wave height were measured. The average monthly temperature, relative humidity, and precipitation values for April 2010 through August 2011 are shown in Figure 4.

The chloride concentration, shown in Figure 4, was measured during an exposure period from May 19, 2010 through August 10, 2011. The measurements taken from Funnels 1 and 2, and then from Funnels 3 and 4, show that the salt deposition was consistent between replicates despite that fact that the two funnels were about 500 feet apart in latitude from one another. Overall, the chloride deposition at the KSC site is high when rated using criteria from the ISO<sup>(5)</sup> 9223 standard,<sup>26</sup> where the highest level of chloride deposition is related to a deposition rate of between 300 and 1500mg/m<sup>2</sup>d. The chloride deposition rate recorded at KSC's beachside test site ranges between 150 and 3500mg/m<sup>2</sup>d, with a weighted mean value of 868mg/m<sup>2</sup>d.

The wave height was monitored because of the relationship between wave height and concentration of marine aerosols, where increased wave height is generally related to an increase in chlorides in the air.<sup>27</sup> Bubbles created from increased wave action are the main generator of marine aerosols<sup>28,29</sup> and

<sup>(5)</sup> International Organization for Standardization, Genève, Switzerland



are generally directly related to wave height. The monthly average wave height for ocean water off the coast of Cape Canaveral and approximately twenty-five miles from the wet candle location was compared to the monthly average chloride concentration to verify the general relationship, shown in Figure 5. The comparison shows that higher wave heights do, in general, correlate directly to increased chloride concentration values, assuming that major weather events, such as hurricanes, are ignored.

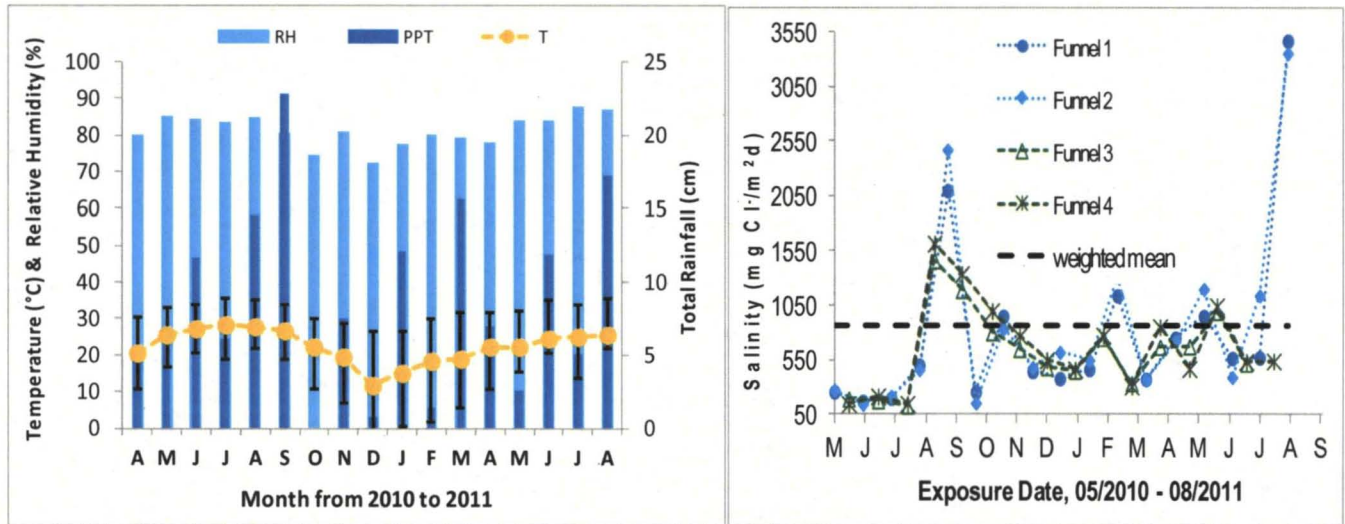


**Figure 4. Average temperature, relative humidity, and precipitation values (left graph), and chloride concentration as a function of exposure period (right graph) from April 2010 to August 2011 recorded at the KSC Beachside Atmospheric Corrosion Test Site.**

Sulfur dioxide concentration was found to be very low at the Kennedy Space Center, with yearly totals ranging from 0.11 to 0.25mg/m<sup>2</sup>-d from 2002 to 2010. A value of less than 4.0mg/m<sup>2</sup>-d is ranked as the lowest level in the ISO 9223 standard for pollution by sulfur-containing substances represented by sulfur dioxide.<sup>26</sup> The yearly total sulfate concentration, SO<sub>4</sub><sup>2-</sup> determined by both wet and dry deposition, was 0.80 to 1.60mg/m<sup>2</sup>-d from 2002 to 2009. The total yearly sulfur concentration, combined wet and dry depositions of sulfur dioxide and sulfates, for the same time period was 0.91 to 1.85mg/m<sup>2</sup>-d. Figure 5 shows the yearly sulfur deposition rates for sulfur dioxide, sulfates (wet and dry deposition), and the combined total.

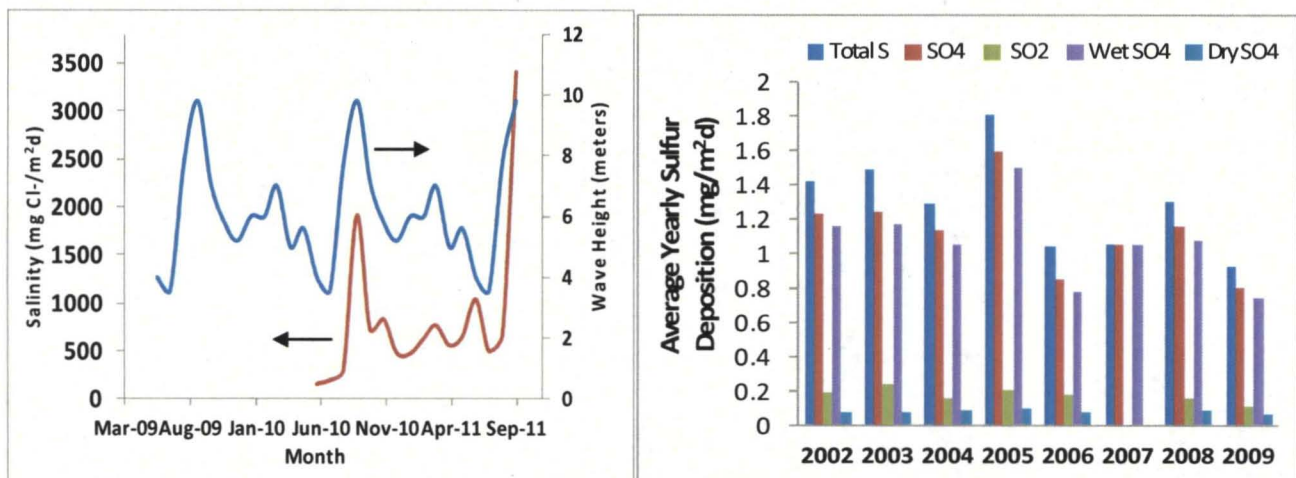


**Figure 5: Average monthly chloride concentration (bottom line) and wave height (top line) (left graph), and sulfur deposition obtained from using both wet and dry deposition methods for collecting sulfur-based contaminants, sulfur dioxide and sulfates (right graph).**



Characterization of atmospheric conditions also involves other factors such as wind, time of wetness, weather events, and UV exposure. This work does not aim to include all the atmospheric factors and uncertainties that exist, but instead to identify them and report on selected atmospheric conditions.

### Corrosion Behavior of 1010 Steel at the Beachside Atmospheric Exposure Site

The corrosion rate of 1010 steel panels exposed at KSC's beach site is variable and dependent on seasonal conditions, as shown in Figure 6. From April 1975 through February 1977 panels were exposed each month for one year, and seasonal changes that influence corrosion rate are evident. Most notable is that panels initially exposed from April through June tend to have an overall lower corrosion rate when compared to the rest of the year, with exceptions for years during major storms (noted in Figure 6). Seasonal variations change from one year to the next. This variability is understandable because, for example, rain patterns can be similar or can vary from one year to the next. An average corrosion rate for 1010 steel panels at KSC is thus difficult to define by one value without considering other seasonal characteristics of the exposure site. Although corrosion rates have been monitored yearly since 2004, they are now being monitored again seasonally starting in 2010 to obtain a more robust data set.

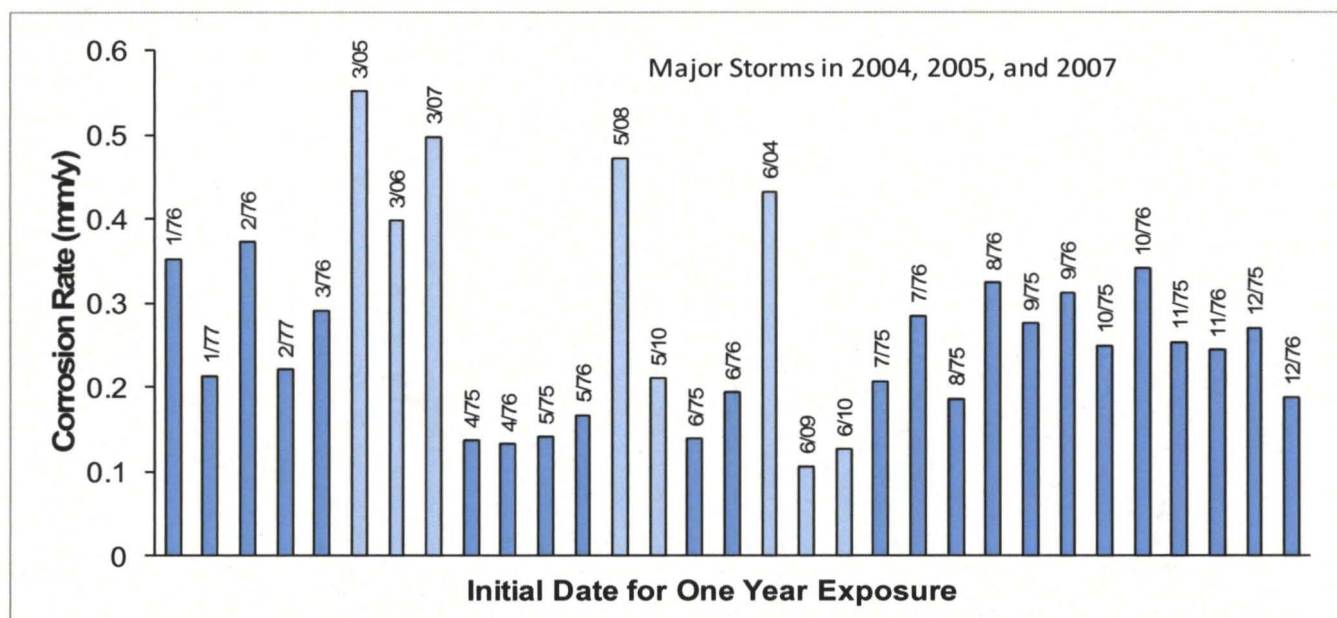


Figure 6: Corrosion rate of 1010 steel panels exposed at the KSC Test Site for one year. Initial exposures are from 4/1975 through 2/1977 (dark fill) and 6/2004 through 6/2010 (light fill).

Corrosion rates of the 1010 steel panels were measured as a function of both monthly and successive monthly exposure times to understand the seasonal characteristics of corrosion rate at KSC. Thus far the corrosion rates, in mm/y, have remained statistically similar throughout the exposure time period from November 2010 to August 2011. Figure 7 shows the corrosion rate and total mass loss of the 1010 steel panels as a function of exposure time. As expected, the panels that were newly exposed each month had a higher overall corrosion rate since corrosion products are not blocking corrosion sites (all areas of the metal surface are available for corrosion). Once corrosion forms on the surface, the corrosion rate generally decreases, as the data in Figure 7 for the successively exposed panels show. The mass loss decreased initially after corrosion product formed across the entire panel surface; however, the mass loss did not diminish as a function of time. The changes in mass loss as a function of exposure time were likely influenced by seasonal factors as well. At this time, it is not possible to fully separate out seasonal and corrosion product influences. The successive corrosion rate monitoring is still ongoing and will continue up to one year.

Seasonal influences on corrosion rates are more evident on the panels exposed monthly and can be compared to the chloride concentration values recorded monthly (Figure 8). While a longer time data set will allow a better comparison in the future, there is a definite direct correlation between the salinity and corrosion rate values thus far. Comparisons were made to monthly corrosion rates and other seasonal characteristics such as temperature and relative humidity. Figure 8 shows that there are direct correlations to relative humidity, corrosion rate, and temperature, where increased moisture (humidity) should provide more time for active corrosion on the steel panel surface. As the temperature increases seasonally and the values of temperature and relative humidity grow closer it is less likely for moisture to form on the panel surface due to humidity alone. Time of wetness will not be discussed in this paper, but is a factor currently being addressed in this study.

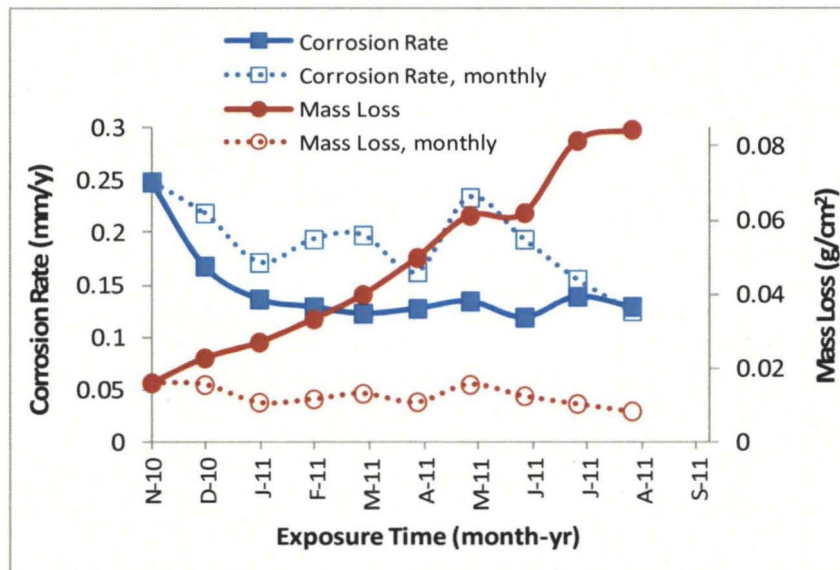


Figure 7: Corrosion rate and mass loss values of 1010 steel panels exposed at the KSC Beachside Atmospheric Test Site and collected monthly and successive monthly.

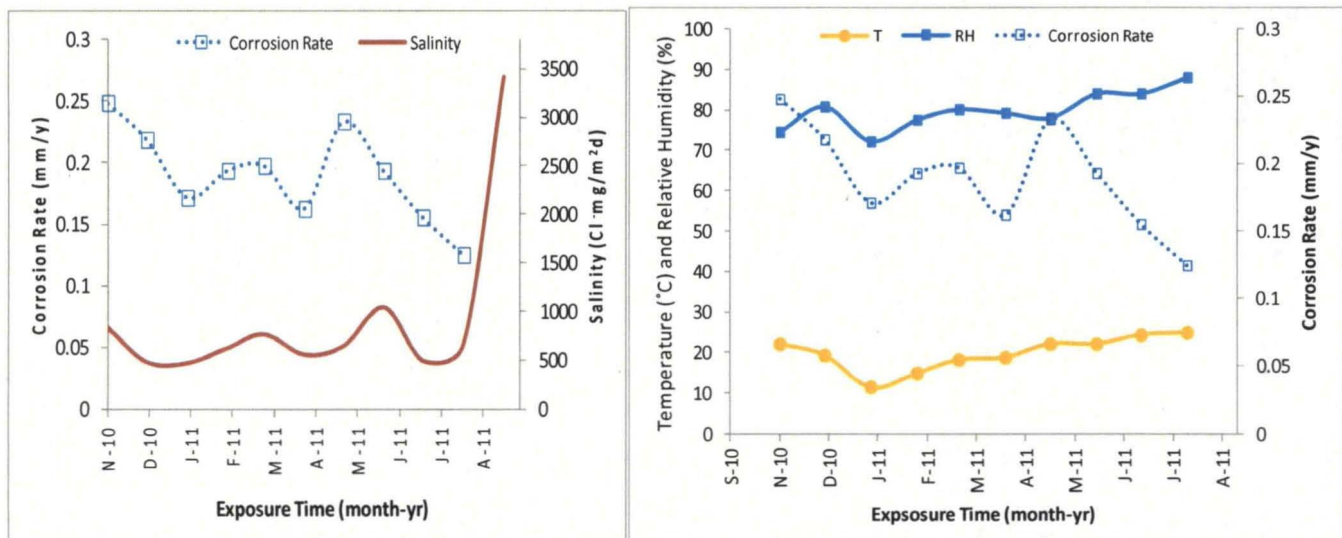


Figure 8: Comparison of corrosion rate and salinity for 1010 steel and wet candles (left graph), and monthly averages for temperature, relative humidity, and corrosion rate recorded at the KSC Beachside Atmospheric Test Site from November 2010 through August 2011 (right graph).



## Correlation of Long-term and Accelerated Corrosion of 1010 Steel

The corrosion rates and behaviors of panels subjected to long-term and accelerated corrosion conditions were compared to identify possible timescale correlations. Corrosion rates for long-term exposure and accelerated corrosion methods, shown in Figure 9 as a function of exposure time, did not correlate because the accelerated conditions tested thus far were too aggressive compared to those of the long-term exposure. Since one primary aim of this work is to find timescale correlations of these accelerated test results to corrosion rates measured after long-term exposure, the corrosion rate values measured in the accelerated tests must be within a reasonable range to match corrosion rates of long-term exposure. Corrosion rate data from the accelerated corrosion test methods are 0.71mm/y and above at low exposure times (30 days for ASST and 4 days or 100 hours for B117) than the highest value of 0.55mm/y obtained from long-term atmospheric exposure. Corrosion rates in mm/y do not seem to be a valuable way to correlate the exposure methods because the accelerated test data, commonly lasting only days or months, is extrapolated to continue at the same linear rate, since the data is normalized at one rate over a year's time. Linear extrapolation of the data leads to false higher rates than actual yearly corrosion rates.

Mass loss values are being used to compare the accelerated methods to long-term corrosion because the metric more clearly shows the different degrees of corrosion as a function of exposure method. Mass loss for panels exposed to salt fog chamber testing occurred at a very consistent rate as a function of exposure time. This is expected since the environmental conditions are consistent throughout the test cycle. The problem with this method is that it is designed to force corrosion at a consistent rate, but it does not take into account the non-linearity of corrosion rates and mass loss in a real-time atmospheric corrosion environment. Although consistent corrosion was induced, the type of corrosion formed in a salt fog chamber is simply too different to be comparable to natural environments.

Mass loss versus timescale behaviors from the ASST and long-term exposure samples are shown in Figure 9. The mass loss of panels exposed to ASST conditions indicated a consistent increase as a function of exposure time, with the exception of exposures less than 60 days long (exposures less than 60 days are currently being examined to confirm correlations at shorter exposure times). The ASST method is designed to accelerate atmospheric corrosion and, as a result, is subject to non-linear corrosion rate and mass loss behaviors.

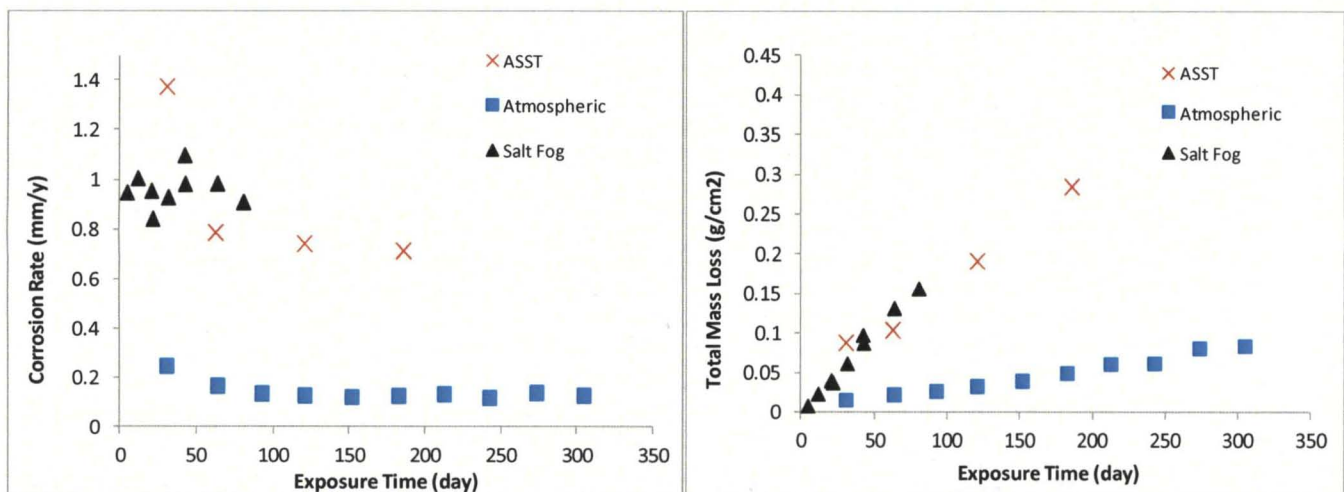


**Figure 9: Comparison of corrosion rates (left graph) and mass loss (right graph) as a function of exposure time for 1010 steel under atmospheric exposure and accelerated corrosion methods.**

Current work is being carried out to analyze whether mass loss rates for long-term exposures can be extrapolated to predict yearly corrosion rates and if ASST mass loss values can be correlated to these predictions. Mass loss correlations cannot, however, be the only factor for correlation. The mechanism



by which the carbon steel panels corrode seems to be markedly different during the long-term and accelerated corrosion conditions. Most significant is that the corrosion products form a much denser layer during the slow atmospheric corrosion process than in the case of either accelerated technique.

During observations of corrosion product formation, distinct differences about the manner in which corrosion formed on the carbon steel surfaces were evident. Panels exposed to atmospheric corrosion have corrosion products that form evenly across the substrate surface, as in the case for general corrosion. Regardless of the amount of moisture that the panels were exposed to each month, the corrosion product still formed evenly across the surface, as shown in Figure 10 for 5 and 55 days of exposure for the same panel. The manner in which the corrosion product formed on the surface directly related to the manner in which moisture was introduced onto the surface of the panel. In the case of atmospheric exposure, the moisture in the form of fog, rain, or dew formed evenly across the surface, and the evaporation rate across the surface also occurred evenly. The ASST panels were exposed to the same atmospheric conditions as the long-term exposure. They also had seawater sprayed directly onto the surface so that the moisture ran across the panels in a continuous vertical stream for 10 minutes of each hour, after which large droplets of seawater remained. The corrosion products formed more heavily in the regions where the seawater remained the longest on the panel surface. Because corrosion rates are known to reach a maximum value during the last stages of moisture film evaporation where oxygen concentration is highest,<sup>30-33</sup> the repeated hourly spray caused the corrosion product to form aggressively especially where the largest droplets formed. Figure 10 shows where corrosion product formed selectively across the surface after one seawater rinse and after 24 rinses. By the 13<sup>th</sup> day of seawater rinsing, the corrosion product had formed more evenly across the same panel surface; however, the corrosion products were formed as prominent surface scales. A distinct vertical build-up of corrosion products formed on the panels in an exaggerated manner as the ASST exposure time increased. During the neutral salt fog exposure the continuous fog caused smaller droplets to collect and eventually stream down the surface of the panels, where the corrosion products then formed most distinctly in the same streaming pattern as the path of the stream of 5-percent sodium chloride solution. The consistently wet conditions produced a rough and flaky corrosion product that did not adhere tightly to the base metal. The backsides of the panels were distinctly uncorroded in many cases. Figure 10 shows examples of this corrosion product formation for the neutral salt fog progressively after 30 minutes, 2 hours, and 100 hours.

The metal surface after prolonged exposure and removal of corrosion products is markedly different for the different corrosion environments. Figure 10 shows examples of the cleaned 1010 steel surfaces, where the interfacial pattern between the corrosion products and metal directly relate to the exposure type as described above. A closer picture of the corrosion products formed after progressive corrosion for long-term atmospheric exposure and compared to neutral salt fog and ASST accelerated methods is shown in Figure 11. The progressive corrosion product formation follows the same pattern as during initial corrosion, as described in the preceding paragraph for each corrosion exposure type. Correlations of corrosion rates and mass losses are evidently more complex when considering these visual comparisons of corrosion product formation.

It is not known whether the visual differences relate to purely physical differences in corrosion product formation or if chemical differences also exist. Although a myriad of iron oxides are known to form during corrosion of carbon steel,<sup>34,35</sup> a question arose as whether different kinds of initial iron oxide corrosion products formed for each corrosion condition since the aggressiveness of each condition varied greatly. Because initial and progressive corrosion products form in generally the same way for each of the corrosion environments, initial corrosion product formation was chosen as a factor related to corrosion method correlation. XPS and microscopy were used to monitor the initial corrosion product formation for each corrosion condition.



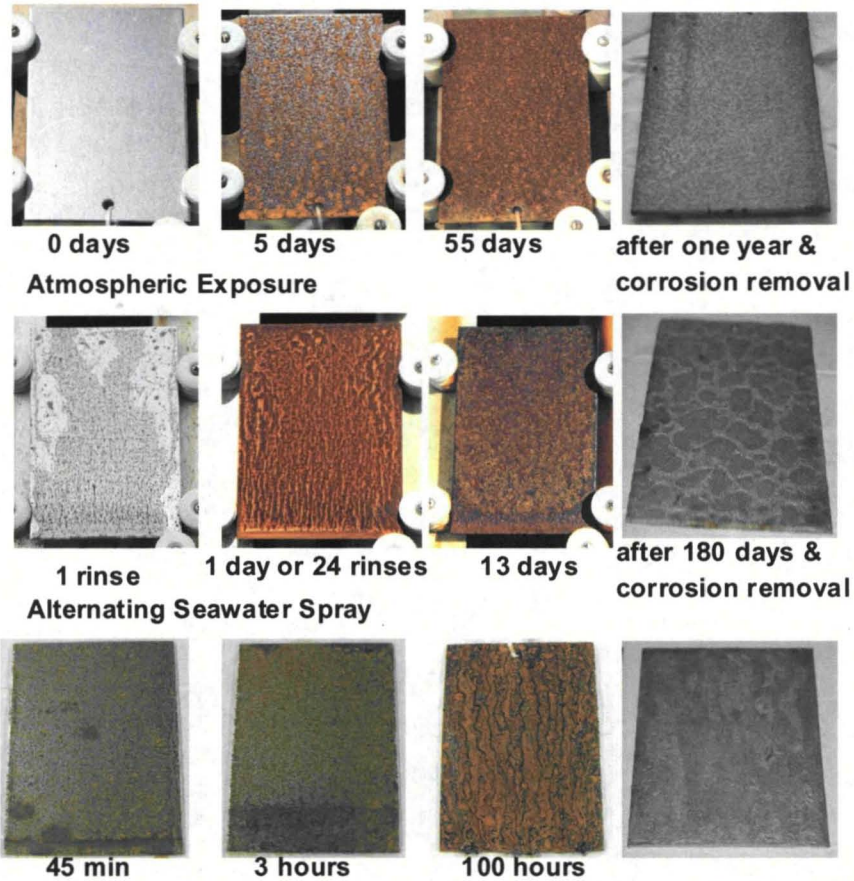


**Figure 10: Examples of 1010 steel (UNS 10100) panels after exposure to atmospheric (top row), alternating seawater spray (middle row), and neutral salt fog (bottom row) corrosion.**



**Figure 11: Examples of 1010 steel (UNS 10100) panels after prolonged exposure to atmospheric (top left), alternating seawater spray (right), and neutral salt fog (bottom left) environments.**

The progression of corrosion as a function of exposure time was markedly different between the panels exposed to beachside atmospheric and each type of accelerated corrosion test method. Again, the corrosion products formed in the same pattern as that in which the moisture (electrolyte) impinged upon the panel surface. The initial corrosion product was monitored each month during atmospheric exposure to identify seasonal differences and include a large range of atmospherically-induced corrosion product types. The atmospherically exposed panels had corrosion that formed initially by local anodic and cathodic reactions that most likely occurred where hygroscopic salts or moisture had



collected. More humid initial conditions meant that the corrosion products formed at a faster rate, but the physical progression, shown in Figure 12, was the same regardless of rate. The panels exposed to neutral salt fog were introduced to a continuous moisture-saturated environment. In this case, the corrosion products first formed at local droplet locations and often at the site where a sodium chloride (NaCl) crystal had formed as Figure 12 shows. The panels used for ASST had initial corrosion product formation in the same pattern as the seawater spray stream that ran down the panel mixed with smaller local corrosion sites that formed during atmospheric exposure, as shown in Figure 12.

Analysis of corrosion products on 1010 steel panels exposed to marine atmospheric corrosion, highlighted in Figure 12 as the targeted analysis points, revealed common features for the iron, carbon, oxygen, and chloride-containing corrosion products. Figure 13 shows that for atmospheric and ASST corrosion environments, the general composition of the 1010 steel surface after initial corrosion was comprised of varying amounts of iron, oxygen, carbon, chloride, sodium, magnesium, manganese, silicon, sulfur, and calcium, depending on the degree of corrosion or the amount of sea salts deposited on the exposed panel. The samples exposed to neutral salt fog included the expected sodium and chloride ions from the sodium chloride solution. All the components, except for iron, oxygen, and carbon, could be accounted for solely by the elements in the exposure environment, while the iron, oxygen, and carbon elements were also components of the base metal. Depth profiling of various points on the panels showed that several shifts resulted during the through-the-thickness transition from corrosion product to iron metal. Figure 14 shows the most general results for a thin layer of initial corrosion product. The iron peaks shift from a surface layer mix of iron(II) chlorides ( $\text{FeCl}_2$ ) and iron oxy-hydroxides ( $\text{FeOOH}$ ) to a thicker layer of bulk iron(III) oxide ( $\text{Fe}_2\text{O}_3$ ) and eventually to the metal surface. This transition always occurred for the iron components regardless of degree of corrosion. However, for thicker corrosion products, the profiling did not always expose the metal surface. The oxygen-based peaks indicated the initial presence of  $\text{FeOOH}$ , as well as the shift to  $\text{Fe}_2\text{O}_3$  during depth profiling. The carbon-based peaks were consistently present, but at varying degrees of intensity through the thickness of the corrosion layer. Different points scanned revealed that chloride-containing carbons, known to naturally occur during degradation of marine aerosol,<sup>36-38</sup> existed on the surface along with elemental carbon. This constituent was confirmed for the chloride peaks, where chlorinated hydrocarbons were notably present along with iron(III) and iron(II) chlorides.

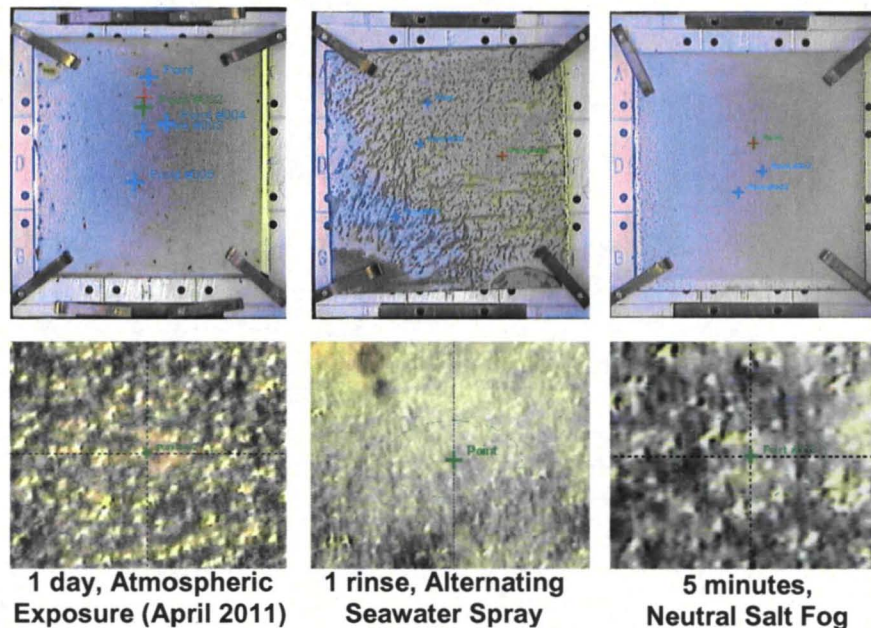


**Figure 12: 1010 steel (UNS 10100) panels after initial exposure to atmospheric, ASST, and neutral salt fog environments. Panels are shown as displayed in the XPS chamber to highlight the points sampled (top row) and the points shown for analysis (bottom row).**



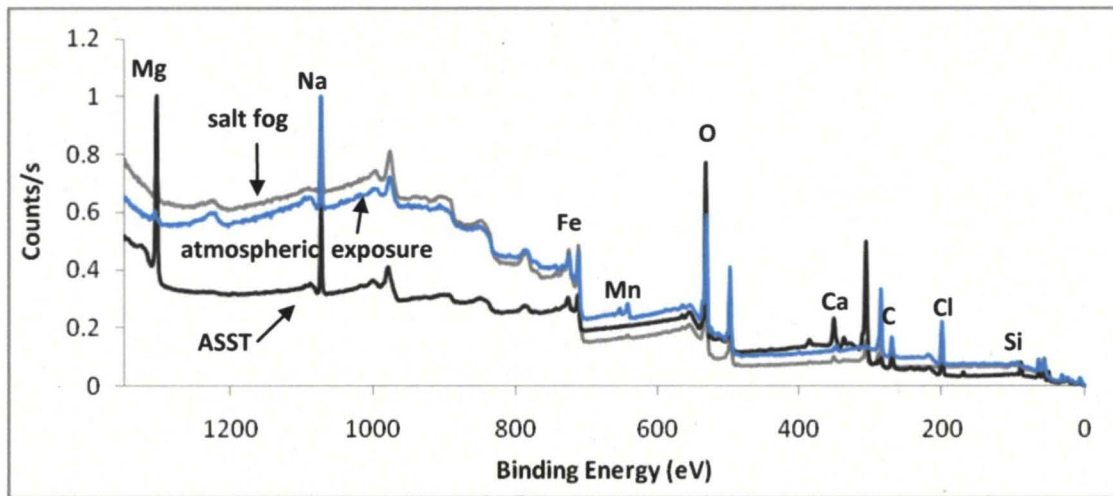


Figure 13: XPS survey spectra of 1010 steel (UNS 1010) panels after initial exposure to atmospheric, ASST, and neutral salt fog environments.

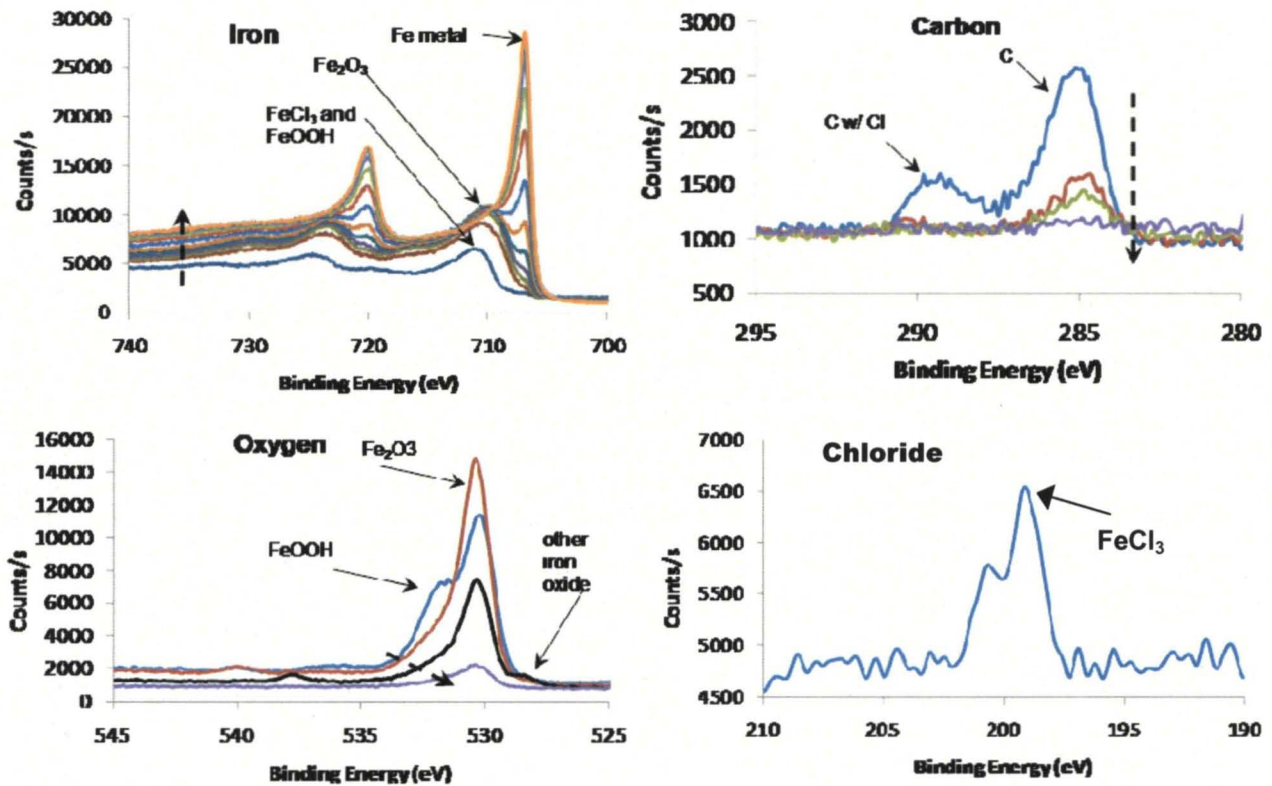


Figure 14: Depth profile results from XPS analysis of 1010 steel (UNS 1010) panels after initial exposure to atmospheric corrosion. The arrows indicate the direction of peak shifting as the depth profiling progressed.



## SUMMARY

Although this work is still in progress, a summary of current results and analysis can be made.

- The Kennedy Space Center's Beachside Atmospheric Corrosion Test Site can be characterized as having high chloride levels between 150 and 3550mg/m<sup>2</sup>d, with a weighted mean value of 868mg/m<sup>2</sup>d, which can be directly related to wave height. The chloride concentration varies seasonally along with other weather conditions such as temperature, humidity, and precipitation. Overall the sulfur dioxide concentrations are very low year-round, estimated to have yearly totals of about 1.0mg/m<sup>2</sup>-d based on 2003 through 2010 data.
- Corrosion rates and mass loss values for the three different 1010 steel exposure techniques: long-term atmospheric, alternating seawater spray, and neutral salt fog are difficult to compare directly since they form corrosion products in different manners. Mass loss as a function of exposure time will be the most reliable way to make correlations between the long-term exposure and accelerated techniques.
- There are distinct physical differences between corrosion products formed under the different exposure techniques. Corrosion products on 1010 steel panels exposed to natural atmospheric conditions at the Kennedy Space Center's Beachside Atmospheric Corrosion Test Site formed slowly and evenly across the panel surfaces. On the panels exposed at the test site and subjected to the Alternating Seawater Spray Test, the initial corrosion products formed aggressively only where the seawater spray settled on the panels. Atmospheric-induced corrosion formed on the rest of the panel, such that the overall corrosion products formed in exaggerated scales across the panel surface. Panels exposed to the neutral salt fog test had corrosion products that initially formed where the droplets collected and later along the streams of moisture that ran down the vertically-oriented panel.
- Despite the physical differences between the corrosion products formed with the different exposure methods, it is unknown at this time if there are chemical differences between the types of iron-based corrosion products formed during initial corrosion of the 1010 steel. This work is in progress.

## ACKNOWLEDGEMENTS

Special thanks to Paul E. Hintze (NASA), Mary C. Whitten (University of Central Florida.), Teddy A. Back, Steven Trigwell, and Jerry Buhrow (ESC-Team QNA) for their technical support.

## REFERENCES

1. G.S. Frankel, "Electrochemical Techniques in Corrosion: Status, Limitations, and Needs", *Journal of ASTM International*, 2008, Vol. 5, 2.
2. B. Boelen, B. Schmitz, J. Defourny, F. Blekkenhorst, "A Literature Survey on the Development of an Accelerated Laboratory Test Method for Atmospheric Corrosion of Precoated Steel Products", *Corrosion Science*, 1993, Vol. 34, 11, p. 1923.
3. Y. Ma, Y. Li, F. Wang, "The Atmospheric Corrosion Kinetics of Low Carbon Steel in a Tropical Marine Environment", *Corrosion Science*, 2010, Vol. 52, p. 1796.



4. E. M. Oliveira, J. R. G. Carneiro, V. F. Cunha Lins, "Evaluation of the Atmospheric Corrosion Resistance of AISI A-36 Steel Painted with Coatings Based on Epoxy and Poly(urethane) Resins Using Semi-accelerated Testing", *Journal of Coating Technology*, 2009, Vol. 6, 2, p. 213.
5. S. Feliu, M. Morcillo and S. Feliu, Jr, "The Prediction of Atmospheric Corrosion from Meteorological and Pollution Parameters- II: Long-Term Forecasts", 1993, Vol. 34, 3, p. 415.
6. S. Feliu, M. Morcillo, S. Feliu, Jr., "The Prediction of Atmospheric Corrosion from Meteorological and Pollution Parameters - I: Annual Corrosion", *Corrosion Science*, 1993, Vol. 34, 3, p. 403.
7. F. Corvo, A.R. Mendoza, M. Autie and N. Betancourt, "Role of Water Adsorption and Salt Content in Atmospheric Corrosion Products of Steel", 1997, Vol. 39, 4, p. 815.
8. H. Schwitzer, H. Bohni, "Influence of Accelerated Weathering on the Corrosion of Low-Alloy Steels", *Corrosion Science*, 1980, Vol. 127, 1, p. 15.
9. E., McCafferty, "Validation of Corrosion Rates Measured by the Tafel Extrapolation Method", *Corrosion Science*, 2005, Vol. 47, 12, p. 3202.
10. Y. Ma, Y. Li, F. Wang, "Corrosion of Low Carbon Steel in Atmospheric Environments of Different Chloride Content", *Corrosion Science*, 2009, Vol. 51, p. 997.
11. J.G. Castaño, C.A. Botero, A.H. Restrepo, E.A. Agudelo, E. Correa, F. Echeverría, "Atmospheric Corrosion of Carbon Steel in Colombia", *Corrosion Science*, 2010, Vol. 52, p. 216.
12. S. Feliu, M. Morcillo, B. Chico, "Effect of Distance from Sea on Atmospheric Corrosion Rate", *Corrosion*, 1999, Vol. 55, 9, p. 883.
13. J.A. Jaen, M.S. de Villalaz, L. de Araque, A. de Bosquez, "Kinetics and Structural Studies of the Atmospheric Corrosion of Carbon Steels in Panama", *Hyperfine Interaction*, 1997, Vol. 110, p. 93.
14. J. Morales, S. Marti'n-Krijer, F. Dí'az, "Atmospheric Corrosion in Subtropical Areas: Influences of Time of Wetness and Deficiency of the ISO 9223 Norm", *Corrosion Science*, 2005, Vol. 47, p.2005.
15. D.M. Drazic, V. Vascic, "The Correlation Between Accelerated Laboratory Corrosion Tests and Atmospheric Corrosion Station Tests on Steel", *Corrosion Science*, 1989, Vol. 29, 10, p. 1197.
16. E.L. Montgomery, L.M. Calle, J.P Curran, and M.R. Kolody, "Timescale Correlation between Marine Atmospheric Exposure and Accelerated Corrosion Testing – an Update," *Department of Defense Corrosion Conference 2011*, La Quinta, CA, July 31- August 5, 2011, paper and presentation.
17. E.L. Montgomery, J.P. Curran, M.R. Kolody, and L.M. Calle, "Timescale Correlation between Marine Atmospheric Exposure and Accelerated Corrosion Testing," *NACE International Corrosion 2011*, Houston, TX, March 13-17, 2011, paper and presentation.
16. G.R. Meira, C. Andrade, C. Alonso, I.J. Padaratz, J.C. Borba, "Modelling Sea-salt Transport and Deposition in Marine Atmosphere Zone – A Tool for Corrosion Studies", *Corrosion Science*, 2008, Vol. 50, p. 2724.
17. J. W. Fitzgerald, "Marine Aerosols: A Review", *Atmospheric Environment*, 1991, Vol. 25A, p. 533.
18. M. Morcillo, B. Chico, L. Mariaca, E. Otero, "Salinity in Marine Atmospheric Corrosion: Its Dependence on the Wind Regime Existing in the Site", *Corrosion Science*, 2000, Vol. 42, p. 91.



19. S. Coburn, "Atmospheric Corrosion Properties and Selection, Carbon Steels", *Metals Handbook*, Metals Park, American Society for Metals, 1978, p. 720.
20. NASA-STD-5008A, "Protective Coating of Carbon Steel, Stainless Steel, and Aluminum on Launch Structures, Facilities, and Ground Support Equipment", 2004.
21. ASTM B117 (latest revision), "Standard Practice for Operating Salt Spray (Fog) Apparatus", *West Conshohocken, PA (ASTM)*.
22. ASTM G1 (latest revision), "Standard Practice for Preparing, Cleaning, and Evaluating Corrosion Test Specimens", *West Conshohocken, PA (ASTM)*.
23. ISO-9225 (latest revision), "Corrosion of Metals and Alloys - Corrosivity of Atmospheres - Measurement of Pollution", (*Geneve, Switzerland ISO*).
- 24 Environmental Protection Agency, <http://java.epa.gov/castnet/viewsiteinfo.do?siteId=IRL14.1>
- 25 National Oceanic and Atmospheric Administration, [http://www.ndbc.noaa.gov/view\\_climplot.php?station=41009&meas=wh](http://www.ndbc.noaa.gov/view_climplot.php?station=41009&meas=wh).
26. ISO-9223 (latest revision), "Corrosion of Metal and Alloys, Corrosivity of Atmospheres - Classification", (*Geneve, Switzerland ISO*).
27. A. Clarke, V. Kapustin, S. Howell, K. Moore, B. Lienert, S. masonis, T. Anderson, D. Covert, "Sea-Salt Size Distributions from Breaking Waves: Implications for Marine Aerosol Production and Optical Extinction Measurements during SEAS", *J. of Atmospheric and Oceanic Technology*, 2003, 20, p1362.
28. M.E.R. Gustafsson and L.G. Franzen, "Inland Transport of Marine Aerosols in Southern Sweden," *Atmospheric Environments*, 2000, 34, 313-325.
29. S.R. Massel, "Ocean Waves Breaking and Marine Aerosol Fluxes," *Atmospheric and Oceanographic Sciences Library*, 2007, Volume 38, p207-228.
30. A. Nishikata, Y. Yamashita, H. Katayama, T. Tsuru, A. Usami, K. Tanabe, H. Mabuchi, "An Electrochemical Impedance Study on Atmospheric Corrosion of Steels in a Cyclic Wet-Dry Condition", *Corrosion Science*, 1995, Vol. 37, 12, p. 2059.
31. F. Mansfeld, "Monitoring of Atmospheric Corrosion Phenomena with Electrochemical Sensors", *Journal of the Electrochemical Society*, 1988, Vol. 135, p. 1354.
32. F. Mansfeld, J.V. Kenkel, "Electrochemical Monitoring of Atmospheric Corrosion Phenomena", *Corrosion Science*, 1976, Vol. 16, p. 111.
33. F. Mansfeld, S. Tsai, "Laboratory Studies of Atmospheric Corrosion - I. Weight Loss and Electrochemical Measurements", *Corrosion Science*, 1980, Vol. 20, p. 853.
34. T.E. Graedel, R.P. Frankenthal, "Corrosion Mechanisms for Iron and Low Alloy Steels Exposed to the Atmosphere", *Journal of the Electrochemical Society*, 1990, Vol. 137, 8, p. 2385.
35. J.T. Keiser, C.W. Brown, "Characterization of the Passive Film Formed on Weathering Steels", *Corrosion Science*, 1983, Vol. 23, 3, p. 251.
36. G.W.Gribble, "Naturally Occurring Organohalogen Compounds - A Comprehensive Survey". *Progress in the Chemistry of Organic Natural Products*, 1996, **68**: 1-423.



37. E.J. Ledet and J.L. Laseter, "Alkanes at the Air-Sea Interface from Offshore Louisiana and Florida," *Science*, 1974, 186, 4, pg 305-314.

38. M. Barbier, D. Joly, A. Saliot, D. Tourres, "Hydrocarbons from Sea Water," *Deep Sea Research Oceanographic*, 1973, 20, 4, pg 305-314.